

Maximal Entanglement in High Energy Physics

Alba Cervera-Lierta,¹ José I. Latorre,^{1,2} Juan Rojo,³ and Luca Rottoli⁴

¹*Dept. Física Quàntica i Astrofísica, Universitat de Barcelona, Diagonal 645, 08028 Barcelona, Spain.*

²*Center for Quantum Technologies, National University of Singapore.*

³*Department of Physics and Astronomy, VU University, De Boelelaan 1081, 1081HV Amsterdam, and Nikhef, Science Park 105, NL-1098 XG Amsterdam, The Netherlands*

⁴*Rudolf Peierls Centre for Theoretical Physics, University of Oxford, 1 Keble Road, Oxford OX1 3NP, UK.*

(Dated: June 9, 2022)

Abstract

We analyze how maximal entanglement is generated at the fundamental level in QED by studying correlations between helicity states in tree-level scattering processes at high energy. We demonstrate that two mechanisms for the generation of maximal entanglement are at work: *i*) s -channel processes where the virtual photon carries equal overlaps of the helicities of the final state particles, and *ii*) the indistinguishable superposition between t - and u -channels. We then study whether *requiring* maximal entanglement constrains the coupling structure of QED and the weak interactions. In the case of photon-electron interactions unconstrained by gauge symmetry, we show how this requirement allows reproducing QED. For Z -mediated weak scattering, the maximal entanglement principle leads to non-trivial predictions for the value of the weak mixing angle θ_W . Our results illustrate the deep connections between maximal entanglement and the fundamental symmetries of high-energy physics.

I. INTRODUCTION

Entanglement [1] is the key property that pervades many developments in quantum physics. As a paramount example, entanglement is necessary to discriminate classical from quantum physics using Bell inequalities [2]. Entanglement can also be understood as the resource that enables genuine quantum protocols such as cryptography based on Bell inequalities [3] and teleportation [4]. Large entanglement is expected to be present in quantum registers when a quantum algorithm produces a relevant advantage in performance over a classical computer such as Shor's algorithm [5]. Entanglement also plays a crucial role in condensed matter, where quantum phase transitions in spin chains are characterized by an enhanced logarithmic scaling of entanglement entropy [6], highlighting the relation between entanglement and conformal symmetry.

It is clear that entanglement is at the core of understanding and exploiting quantum physics. It is therefore natural to analyze the generation of entanglement at its most fundamental origin, namely the theories of fundamental interactions in particle physics. If the quantum theory of electromagnetism, QED, would never generate entanglement among electrons, Nature would never display a violation of a Bell inequality. This implies that entanglement must be generated by quantum unitary evolution at the more fundamental level.

A deeper question emerges in the context of high-energy physics. Is maximal entanglement (MaxEnt) possible at all? In other words, are the laws of Nature such that MaxEnt can always be realized? One can imagine a QED-like theory where entanglement could be generated, but in a way which would be insufficient to violate Bell inequalities. Then, it would be formally possible to think of the existence of an underlying theory of hidden variables. On the other hand, if MaxEnt is realized in QED, it is then possible to design experiments that will discard classical physics right at the level of scattering of elementary particles. Taking a step further, one can ask what are the consequences of imposing that the laws of Nature must be able to realize maximally entangled states. Can this requirement be promoted to a principle, and to which extent is it consistent with fundamental symmetries such as gauge invariance?

Here we will show first than in QED only two mechanisms can generate MaxEnt in high-energy scattering of fermions prepared in an initial helicity product state. These are *i*) s -channel processes where the virtual photon carries equal overlaps of the helicities of the final state particles, and *ii*) processes which display interference between t and u channels. We will then illustrate the deep connection between maximal entanglement and the structure of the electron-photon interaction vertex in QED. We shall finally analyze the consequences of imposing MaxEnt on the weak interactions.

Notice that in two-particle systems the concepts of maximal entanglement and maximal entropy are equivalent, as the reduced density matrix for any of the two particles is proportional to the identity, which is the maximally entropic state. For systems with more than two particles, the classification of entanglement becomes richer and does not necessarily correspond to the entropy of the system. As in this work we focus only on processes with two particles, we shall use MaxEnt to refer indistinctly to maximal entanglement or maximal entropy.

Some previous works have studied the role of entanglement in particle physics. In Ref. [7] it was shown that orthopositronium can decay into 3-photon states that can be used to perform Bell-like experiments that discard classical physics faster than the standard 2-particle Bell inequality. Bell inequalities have also been discussed in kaon physics [8] and its relation with the characterization of T -symmetry violation [9] as well as in neutrino oscillations [10]. How entanglement varies in an elastic scattering process has been studied using the S -matrix formalism in [11]. Note also recent work on entanglement in Deep Inelastic Scattering [12]. Also, a discussion of quantum correlations in the CMB radiation has been brought to the domain of Bell inequalities [13].

The outline of this paper is as follows. In Sect. II we introduce measures to quantify entanglement in scattering processes. Then in Sect. III we study how entanglement is generated in QED scattering processes. In Sect. IV we investigate to which extent MaxEnt can be used as constraining principle on the structure of the QED interactions. Finally, in Sect. V we assess some of the implications of MaxEnt for the weak interactions, and in Sect. VI we conclude. A number of technical details of the calculations are collected in the appendices: App. A, about QED scattering amplitudes with helicity dependence; App. B, about unconstrained QED; and App. C, about helicity-dependent calculations in electroweak theory.

II. QUANTIFYING ENTANGLEMENT

We shall study here scattering processes involving fermions and photons as incoming and outgoing particles. In the case of fermions (photons) we shall analyze the entanglement of their helicities (polarizations). In both cases, the associated Hilbert space is two-dimensional, and we use $|0\rangle$ and $|1\rangle$ as basis vectors. The quantum state of an incoming or outgoing particle can then be written as

$$|\phi\rangle = \alpha|00\rangle + \beta|01\rangle + \gamma|10\rangle + \delta|11\rangle, \quad (1)$$

where $|\alpha|^2 + |\beta|^2 + |\gamma|^2 + |\delta|^2 = 1$ due to normalization. We note that in high-energy scattering a generic outgoing state will involve all possible outcomes of the process being analyzed. The reduction to a two-level system therefore corresponds to a post-selection of results. This is the correct description that delivers the probabilities which we could insert into a Bell inequality, once the final state has been identified.

To quantify entanglement we could use the Von Neumann entropy, but this is not necessary since in our case all possible entanglement measures are related to

$$\Delta \equiv 2|\alpha\delta - \beta\gamma|, \quad (2)$$

known as the *concurrence* [14]. By construction, $0 \leq \Delta \leq 1$, where the extreme cases $\Delta = 0$ (1) correspond to a product (maximally entangled) state.

Here we shall study scattering process where the incoming particles are in a product state of their helicities, that is, the incoming particles are not entangled ($\Delta = 0$). We will often work in the high energy limit where helicities and chirality are equivalent, and we will use the basis $|0\rangle_{\text{in}} = |R\rangle$ and $|1\rangle_{\text{in}} = |L\rangle$, where R and L correspond to right- and left-handed helicities. In general, the outgoing state will be a superposition of all possible helicity combinations, and thus the scattering amplitude of e.g. RL initial helicities, \mathcal{M}_{RL} , will include each possible combination of outgoing helicities. We will then parametrize scattering amplitudes as

$$\mathcal{M}_{RL} \sim \alpha_{RL}|RR\rangle + \beta_{RL}|RL\rangle + \gamma_{RL}|LR\rangle + \delta_{RL}|LL\rangle, \quad (3)$$

where here RL stand for the incoming helicities, and the kets indicates the values of the outgoing ones.

III. MAXENT GENERATION IN QED

Let us start our discussion with the analysis of how entanglement is generated in electron-positron annihilation into a muon-antimuon pair, $e^-e^+ \rightarrow \mu^-\mu^+$, described at tree level in QED by a single s -channel diagram. In order to analyze entanglement, it is necessary to retain all the helicities in the calculation. As in the rest of this paper, we will work on the center-of-mass frame.

It is convenient to first focus on the current generated at the interaction vertices. If the incoming particles propagate along the z -direction, the incoming current associated to two incoming particles in a RL helicity product state will be $\bar{v}_\uparrow \gamma^\mu u_\uparrow = 2p_0(0, 1, i, 0)$, where p_0 is the electron's energy. The outgoing particles will be described by a current as a function of θ , the scattering angle. As shown in the appendix, we find that at high energies the leading contribution only appears for incoming RL (and LR) helicities,

$$\mathcal{M}_{RL} \sim (1 + \cos\theta)|RL\rangle + (-1 + \cos\theta)|LR\rangle \quad (4)$$

up to a prefactor which is not relevant here. Thus for a scattering angle $\theta = \pi/2$ the final state becomes maximally entangled and proportional to $|RL\rangle - |LR\rangle$, with $\Delta_{RL} = 1$. This result illustrates how MaxEnt can be generated in a high-energy scattering process. While scattering amplitudes in general carry a non-trivial angular dependence, it is always possible to perform the measurement in the specific direction where MaxEnt is obtained, not unlike the way maximally entangled states are obtained in quantum optics by parametric down conversion. Let us also note that the dominant terms in the $e^-e^+ \rightarrow \mu^-\mu^+$ scattering at high energies are easily described by chirality conservation. This is not the case at lower energies, where the emergence of entanglement is more elaborated.

For incoming particles in the RR helicity product state, all terms in the amplitude are suppressed by a power of p_0 as compared to the RL case. Nevertheless, MaxEnt is found for every angle θ and incoming momenta p^0 . An experiment that prepares RR incoming states will therefore always result in MaxEnt.

It is instructive to revisit the computation of the RL case focusing on the currents associated to the virtual photon. The incoming current (in the z -direction) corresponds to $j_{\text{in}}^{\mu(RL)} = 2p_0(0, 1, i, 0)$, and at high energies the non-vanishing outgoing currents at $\theta = \pi/2$ read $j_{\text{out}}^{\mu(RL)} = 2p_0(0, 0, -i, -1)$ and $j_{\text{out}}^{\mu(LR)} = 2p_0(0, 0, i, -1)$. Thus the third component of j_{in} carries equal overlap (with different sign) of the two possible helicity combinations for the outgoing state. In a sense, the photon cannot distinguish between those two options. This is the basic element that leads to MaxEnt generation in s -channel processes.

Entanglement can also be generated in QED through a completely different mechanism. Let us consider Møller (electron-electron elastic) scattering, which receives contributions only from t - and u -channel diagrams. For this process, the computation of the amplitude shows that no entanglement is generated at high energies within each t or u channel separately, and that the only entangled state is produced by their superposition, resulting in $\mathcal{M}_{RL} \sim (t/u)|LR\rangle - (u/t)|RL\rangle$, leading to a concurrence

$$\Delta_{RL} \xrightarrow{p_0 \rightarrow \infty} 2 \frac{u^2 t^2}{u^4 + t^4} \xrightarrow{t=u} 1. \quad (5)$$

Therefore MaxEnt ($\Delta_{RL} = 1$) is realized when $t = u$, which corresponds again to the scattering angle being $\theta = \pi/2$. The indistinguishability of u and t histories is now at the heart of entanglement. This also implies that entanglement will not be generated in processes such as $e^-\mu^- \rightarrow e^-\mu^-$ where the same u/t interference cannot take place. Including electron mass m_e effects, the concurrence Δ_{RL} reads

$$\left| \frac{2tu \left(tu + m_e^2 \frac{(t-u)^2}{t+u} \right)}{2m_e^2(t-u)^2(2m_e^2 - 2(t+u) + \frac{tu}{t+u}) + (t^4 + u^4)} \right|, \quad (6)$$

which shows the more powerful result that, for all energies, the scattering angle $\theta = \pi/2$ (when $t = u$) leads to MaxEnt, $\Delta_{RL}|_{\theta=\pi/2} = 1$ for all p_0 .

In the case of incoming particles in an RR product state, no entanglement is generated in the high-energy limit, since the amplitude is dominated by the final state which also lives in the RR sector, as required by helicity conservation. At very low energies on the other hand, the calculation of the concurrence gives

$$\Delta_{RR} \xrightarrow{|\vec{p}| \ll m_e, \theta = \pi/2} 1 + O(|\vec{p}|^2/m_e^2). \quad (7)$$

The combination of Eqns. (5) and (7) illustrates the remarkable fact that two electrons will get always entangled at low energies, irrespective of their initial helicities.

The way in which MaxEnt is generated in QED scattering processes can be studied more thoroughly. It is indeed possible to show that MaxEnt also arises in Bhabha scattering and in pair annihilation of electron-positron to two photons. Table I shows the MaxEnt states that can be obtained in all tree-level QED processes, both at high and low energies. All processes, with the exception of electron-muon scattering and Compton scattering (photon-electron scattering) can generate maximally entangled states in some energy limit and at a given scattering angle. In two cases, MaxEnt is generated independently of the center of mass angle: pair annihilation into photons, and electron-positron annihilation into muons, in both cases at low energy and for an initial state $|RR\rangle$. It is highly non-trivial that a single coupling, the QED vertex, can take care of generating entanglement in all these processes, and at the same time guarantee that if entanglement is present in the initial state, it will be preserved by the interaction.

IV. MAXENT AS A CONSTRAINING PRINCIPLE

It is tantalizing to turn the discussion upside down and attempt to promote MaxEnt to a fundamental principle that constraints particle interactions. Such principle would guarantee the intrinsically quantum character of the

	Initial state $ RR\rangle$		Initial state $ RL\rangle$	
	High Energy	Low Energy	High Energy	Low Energy
$e^- \mu^- \rightarrow e^- \mu^-$	–	–	–	–
$e^- e^+ \rightarrow \mu^- \mu^+$	–	$(\cos \theta \Phi^- \rangle - \sin \theta \Psi^+ \rangle)_{\vee \theta}$	$ \Psi^- \rangle_{\theta=\pi/2}$	–
$e^- e^- \rightarrow e^- e^-$	–	$ \Phi^- \rangle_{\theta=\pi/2}$	$ \Psi^- \rangle_{\theta=\pi/2}$	$ \Psi^- \rangle_{\theta=\pi/2}$
$e^- e^+ \rightarrow e^- e^+$	–	–	$ \Psi^+ \rangle_{\theta=\pi/2}$	–
$e^- e^+ \rightarrow \gamma \gamma$	–	$ \Phi^- \rangle_{\vee \theta}$	$ \Psi^- \rangle_{\theta=\pi/2}$	–

	Initial state $ R+\rangle$		Initial state $ R-\rangle$	
	High Energy	Low Energy	High Energy	Low Energy
$e^- \gamma \rightarrow e^- \gamma$	–	–	–	–

TABLE I: Maximally-entangled states ($\Delta = 1$) for tree-level QED processes, both in the high- and low-energy limits. The states are written in terms of the Bell basis, $|\Phi^\pm\rangle \sim |RR\rangle \pm |LL\rangle$ and $|\Psi^\pm\rangle \sim |RL\rangle \pm |LR\rangle$. For the processes in the upper part of the table, the initial state is expressed in terms of the helicities of the fermions, R and L . For Compton scattering, $e^- \gamma \rightarrow e^- \gamma$, the initial state is expressed in terms of the helicity of the electron and the polarization of the photon, $|+\rangle$ or $|-\rangle$. The scattering angle where the entangled state is produced is indicated in the subscript.

laws of Nature, allowing Bell-type experiments to be carried out violating the bounds set by classical physics. In this formulation, MaxEnt emerges as a purely information-theoretical principle that can be applied to a variety of problems.

We shall further explore this idea in the context of an unconstrained version of QED (uQED). This is a theory of fermions and photons, obeying the Dirac and Maxwell equations respectively, which can interact via a generic vertex that allows violations of rotation and gauge invariance. For simplicity we shall still impose the C, P and T discrete symmetries. While of course this theory is not realized in Nature, our goals are to determine to which extent imposing MaxEnt constrains this interaction vertex and to verify that QED can be reproduced.

To be specific, we shall replace the QED vertex $e\gamma^\mu$ with a general object eG^μ that can be expanded in a basis of 16 4×4 matrices. This unconstrained interaction vertex can be parametrized as $G^\mu = a_{\mu\nu} \gamma^\nu$, where $a_{\mu\nu}$ are real numbers and $a_{0j} = a_{i0} = 0$ for $i, j = 1, 2, 3$. The QED vertex is recovered for $a_{00} = a_{11} = a_{22} = a_{33} = 1$ and $a_{ij} = 0$ for $i \neq j$. The computation of the amplitude $\mathcal{M}_{RL \rightarrow RL/LR}$ for $e^- e^+ \rightarrow \mu^- \mu^+$ scattering in uQED at high energies gives

$$\mathcal{M}_{RL} \sim (a_{j1} + ia_{j2})(a_{j1} \cos \theta \mp ia_{j2} - a_{j3} \sin \theta), \quad (8)$$

where the $-(+)$ sign corresponds to the $RL(LR)$ final state helicities and the sum over j is understood. By requiring that MaxEnt is realized in the form $|RL\rangle - |LR\rangle$ ($\Delta_{RL} = 1$) at $\theta = \pi/2$ we derive the constraint $(a_{j1} + ia_{j2})a_{j3} = 0$. Introducing the positive-defined Hermitian matrix $A_{kl} = a_{kj} a_{lj}$, this condition implies $A_{13} = A_{23} = 0$, consistent with QED where all $a_{ij} = 0$ for $i \neq j$. While in general it is not justified to assume that MaxEnt in uQED emerges for the same θ as in QED, this example shows the constraints which are obtained from concurrence maximization.

Let us notice that the uQED formalism allows angular momentum violation. For instance, let us consider the process $e^+ e^- \rightarrow \mu^+ \mu^-$, and take $\theta = \pi/2$ and $a_{13} = a_{23} = a_{33} = 0$. If the initial state is $|\Psi^- \rangle = \frac{1}{\sqrt{2}} (|RL\rangle - |LR\rangle)$, i.e. the singlet state, then the final state is proportional to $|RL\rangle + |LR\rangle$, and therefore violates angular momentum conservation (see Appendix B for more details).

The complete application of the MaxEnt principle to uQED requires the computation of all the scattering amplitudes in the new theory and then the determination of the constraints on the $a_{\mu\nu}$ coefficients from the maximization of the concurrences. Here we have maximized the sum of the concurrences of four different processes: Bhabha and Møller scattering, $ee \rightarrow \gamma\gamma$ and $e^- e^+ \rightarrow \mu^- \mu^+$, accounting for all initial helicity combinations for product states. The maximization has been performed both over the $a_{\mu\nu}$ coefficients and over the scattering angle θ . Full consistency is found between the constraints provided by each of the four processes. The solution to the maximization of the concurrence is found to be

$$(G^0, G^1, G^2, G^3) = (\pm\gamma^0, \pm\gamma^1, \pm\gamma^2, \pm\gamma^3), \quad (9)$$

which shows that QED is indeed a solution (though not the only one) of requiring MaxEnt for the above subset of

scattering processes in uQED. Some of these solutions are equivalent to QED since a global sign can be absorbed in the electric charge.

The solutions Eq. (9) are divided into two groups, those related to QED and those that are inconsistent with QED, for instance because they violate rotation symmetry. The latter solutions cannot be ruled out since the scattering processes considered here cannot determine the overall sign of the γ^μ matrices, as they always appear in pairs. Including further scattering or decay processes which involve three outgoing particles might remove this ambiguity and eliminate the inconsistent solutions.

V. MAXENT IN THE WEAK INTERACTIONS

The mechanism underlying MaxEnt generation in weak interactions is more subtle, due to the interplay between vector and axial currents and between Z and γ channels. The coupling of the Z boson to fermions reads

$$i \frac{g}{\cos \theta_W} \gamma^\mu \left(g_V^f - g_A^f \gamma^5 \right), \quad (10)$$

where the axial and vector couplings are $g_A^f = T_3^f/2$ and $g_V^f = T_3^f/2 - Q_f \sin^2 \theta_W$, and θ_W is the Weinberg mixing angle. For electrons and muons, $T_3 = -1/2$ and $Q_f = -1$. Beyond tree level, the Weinberg angle runs with the energy and is scheme dependent. The PDG average [15] at $Q = m_Z$ in the on-shell scheme is $\sin^2 \theta_W \simeq 0.2234$. In the Standard Model (SM) thus we have that for electrons the vector coupling $|g_V|$ is smaller than the axial one $|g_A|$ by about order of magnitude.

Accounting for the effects of the new axial component in the fermion-boson coupling can be done as follows. We first consider $e^- e^+ \rightarrow \mu^- \mu^+$ scattering mediated by a Z boson in the high energy limit, where m_Z is neglected. We define *left* and *right* couplings as $g_L = g_V + g_A$ and $g_R = g_V - g_A$, which simplifies the structure of the currents since $j_{\text{in}}^{RL} \sim g_R(0, 1, i, 0)$ and $j_{\text{in}}^{LR} \sim g_L(0, 1, -i, 0)$. The resulting scattering amplitudes are:

$$\begin{aligned} \mathcal{M}_{LR} &\sim (1 + \cos \theta) g_L^2 |LR\rangle + (-1 + \cos \theta) g_L g_R |RL\rangle, \\ \mathcal{M}_{RL} &\sim (-1 + \cos \theta) g_R g_L |LR\rangle + (1 + \cos \theta) g_R^2 |RL\rangle, \end{aligned} \quad (11)$$

and their concurrences for $|\vec{p}| \gg m_Z$ read:

$$\Delta_{LR(RL)} \simeq \frac{\sin^2 \theta |g_L g_R|}{2(c^4 g_L^2 + s^4 g_R^2)} \left(\frac{\sin^2 \theta |g_L g_R|}{2(s^4 g_L^2 + c^4 g_R^2)} \right), \quad (12)$$

where $c = \cos \theta/2$ and $s = \sin \theta/2$ depend on the scattering angle θ . Applying the MaxEnt requirement to the concurrences Eq. (12) we derive a constraint between the couplings g_R and g_L and θ , namely $c^2 g_L \pm s^2 g_R = 0$ ($s^2 g_L \pm c^2 g_R = 0$) for the LR (RL) initial states. Note that in general concurrence maximization occurs for different values of θ for each initial state. This result can be traced back to the $Z \rightarrow f \bar{f}$ decay, and indeed the decay of any polarization of the Z particle gets maximally entangled under the condition $\sin^2 \theta_W = 1/4$. Thus scattering processes mediated by a Z inherit the entanglement structure from Z decays.

In Fig. 1 we show the maximal concurrence lines ($\Delta = 1$) as a function of the scattering angle θ and of the coupling ratio g_R/g_L for the two combinations LR and RL . We find that both concurrences are simultaneously maximized for $\theta = \pi/2$, where $g_R = \pm g_L$, that is, either $g_A = 0$ or $g_V = 0$. If the axial coupling vanishes $g_A = 0$, we recover the known QED result. The $g_V = 0$ solution, a vanishing vector coupling, corresponds to a Weinberg angle of $\sin^2 \theta_W = 1/4$, in agreement with the experimental value at the Z pole [15] within $\sim 10\%$. There are two possible explanations for such a discrepancy. On the one hand, this analysis has been performed at first order in perturbation theory; the full MaxEnt analysis should be performed taking into account also higher orders, which modify the amplitudes. On the other hand, it is possible that MaxEnt does not fix this parameter, but only gives us a close value, a first intuition. It is however remarkable that requesting MaxEnt simultaneously for the two initial state helicities leads either to QED or to a theory which looks surprisingly close to the weak interaction.

We have also studied how this result is modified if we include the contribution from γ exchange, a non-trivial check since this adds terms to both RL and LR which are independent of $\sin^2 \theta_W$, finding that while the angular dependences are modified the MaxEnt predictions are preserved. While the application of MaxEnt to Z -boson mediated scattering does not fix completely the coupling structure of the weak interactions, as we mentioned its application to Z decay fixes $g_V = 0$ and thus $\sin^2 \theta_W = 1/4$. The lack of full predictivity of MaxEnt in the full scattering case is due to the freedom to choose different angles for MaxEnt depending on the chirality of the initial particles.

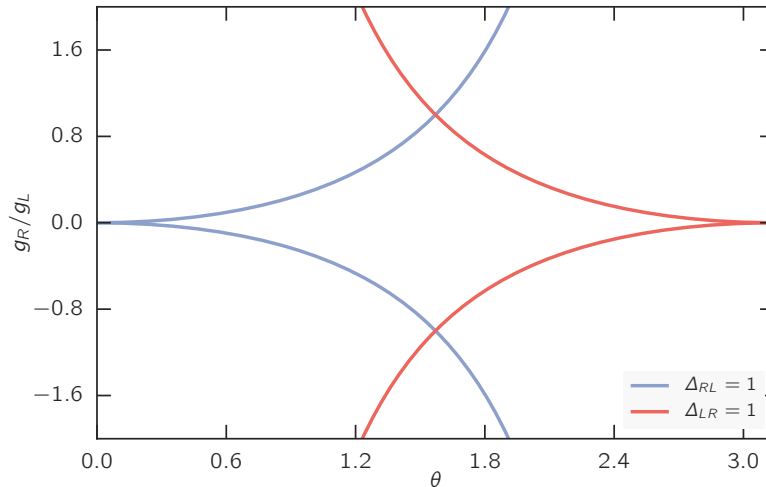


FIG. 1: Maximal concurrence line as a function of the angle θ and the coupling ratio g_R/g_L for Z -mediated $e^-e^+ \rightarrow \mu^-\mu^+$ scattering for the LR and RL initial state helicities.

VI. SUMMARY

Fundamental interactions generate entangled states using mechanisms based on indistinguishability, consistently with the symmetries of the theory. In this work we have explored the relationship between maximally entangled states and high energy scattering amplitudes in QED and the weak interactions. We found that promoting MaxEnt to a fundamental principle allows one to constrain the coupling structure describing the interactions between fermions and gauge bosons. We also found that MaxEnt in the weak interactions prefers a weak angle $\theta_W = \pi/6$, surprisingly close to the SM value. In the “*It from Qubit*” viewpoint of J. A. Wheeler, where “*all things physical are information-theoretic in origin*” [16], the fundamental particle interactions represent a set of operations to implement basic information ideas and protocols. In this framework, MaxEnt arises as a possible powerful information principle that can be applied to different processes, bringing in unexpected important constraints on the structure of high-energy interactions. It is conceivable that extensions of the MaxEnt principle to other processes will lead to new insights in the structure of the SM or on theories of New Physics beyond it.

Acknowledgements

We thank our colleagues L. Álvarez-Gaumé and C. Gómez for fruitful discussions. L. R. thanks E. Nocera for useful discussions. A. C. is grateful to the University of Oxford for hospitality.

a. Funding information A. C. and J. I. L. acknowledge support from FIS2015-69167-C2-2-P project. The work of J. R. and L. R. is supported by the ERC Starting Grant “PDF4BSM”.

Appendix A: QED scattering amplitudes with helicity dependence

In this appendix we provide explicit results for the calculations of some of the relevant QED scattering amplitudes with explicit helicity dependence. Specifically, we consider electron-positron annihilation into muons, Møller scattering, and pair annihilation into photons.

1. Electron-positron annihilation into muons: $e^-e^+ \rightarrow \mu^-\mu^+$

The first QED process that we consider is electron-positron annihilation into muons, $e^-e^+ \rightarrow \mu^-\mu^+$. At Born level, there is a single Feynman diagram that contributes to the amplitude, and is shown in Fig. 2. This scattering process is mediated by a virtual photon in the s channel. We are interested in computing the scattering amplitudes for initial and final states with well defined helicities. Up to an overall factor which is irrelevant for the discussion of

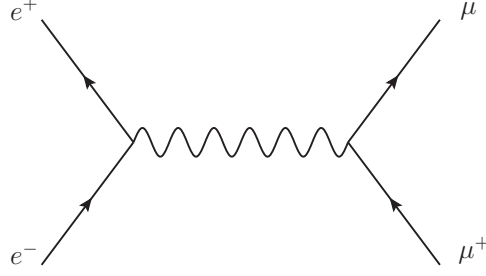


FIG. 2: Feynman diagram for electron-positron scattering into a muon-antimuon pair at tree level.

entanglement, for the case of where the initial product state shares the same helicities, these amplitudes are given by

$$\begin{aligned}
 \mathcal{M}_{|RR\rangle\rightarrow|RR\rangle} &= -\mathcal{M}_{|RR\rangle\rightarrow|LL\rangle} = -\frac{\lambda}{\mu^2 + \lambda^2} \cos \theta, \\
 \mathcal{M}_{|RR\rangle\rightarrow|RL\rangle} &= \mathcal{M}_{|RR\rangle\rightarrow|LR\rangle} = \frac{\lambda}{\sqrt{\mu^2 + \lambda^2}} \sin \theta, \\
 \mathcal{M}_{|LL\rangle\rightarrow|RR\rangle} &= -\mathcal{M}_{|LL\rangle\rightarrow|LL\rangle} = \frac{\lambda}{\mu^2 + \lambda^2} \cos \theta, \\
 \mathcal{M}_{|LL\rangle\rightarrow|RL\rangle} &= \mathcal{M}_{|LL\rangle\rightarrow|LR\rangle} = -\frac{\lambda}{\sqrt{\mu^2 + \lambda^2}} \sin \theta,
 \end{aligned} \tag{A1}$$

and in the case where the input product state has different helicities,

$$\begin{aligned}
 \mathcal{M}_{|RL\rangle\rightarrow|RR\rangle} &= -\mathcal{M}_{|RL\rangle\rightarrow|LL\rangle} = -\frac{\sin \theta}{\sqrt{\mu^2 + \lambda^2}}, \\
 \mathcal{M}_{|LR\rangle\rightarrow|RR\rangle} &= -\mathcal{M}_{|LR\rangle\rightarrow|LL\rangle} = -\frac{\sin \theta}{\sqrt{\mu^2 + \lambda^2}}, \\
 \mathcal{M}_{|RL\rangle\rightarrow|RL\rangle} &= -(1 + \cos \theta), \\
 \mathcal{M}_{|RL\rangle\rightarrow|LR\rangle} &= (1 - \cos \theta), \\
 \mathcal{M}_{|LR\rangle\rightarrow|RL\rangle} &= (1 - \cos \theta), \\
 \mathcal{M}_{|LR\rangle\rightarrow|LR\rangle} &= -(1 + \cos \theta),
 \end{aligned} \tag{A2}$$

where θ is the scattering angle in the center of mass frame, $\lambda \equiv m_e/m_\mu$ is the ratio between the electron and muon mass, and $\mu \equiv |\vec{p}|/m_\mu$ is the ratio of the momentum of the incoming electrons over the muon mass. In the high energy limit, where the center of mass energy of the scattering is much larger than the muon mass, we have that $\mu \rightarrow \infty$. In this limit it is also of course a very good approximation to assume that $\lambda \ll \mu$. In this limit, we see from Eq. (A2) that all the scattering amplitudes involving fermions of the same helicity either in the initial or in the final state are subleading, and the dominant amplitudes are those where both the initial and final states are composed by particles with different helicity.

Using the concurrence, Eq. (2), to quantify the amount of entanglement between the helicities of the outgoing particles present in each of these scattering processes, we obtain that for a generic value of the center-of-mass energy μ we have

$$\Delta_{RR} = 1, \tag{A3}$$

$$\Delta_{RL} = \frac{(\mu^2 + \lambda^2 - 1) \sin^2 \theta}{(\mu^2 + \lambda^2)(1 + \cos^2 \theta) + \sin^2 \theta}. \tag{A4}$$

Therefore, for RR scattering there is always maximally entangled, for any energy. The same is true for LL scattering. Note that in the high-energy limit however the contribution to the RR and LL initial helicity states is suppressed by a factor $1/\mu$ with respect to the RL and LR combinations, and thus will contribute much less to the total cross section.

The high-energy limit for the RL concurrence reads

$$\Delta_{RL} \xrightarrow{\mu \rightarrow \infty} \frac{\sin^2 \theta}{1 + \cos^2 \theta} + \mathcal{O}\left(\frac{1}{\mu^2}\right) \xrightarrow{\theta \rightarrow \pi/2} 1 + \mathcal{O}\left(\frac{1}{\mu^2}\right). \tag{A5}$$

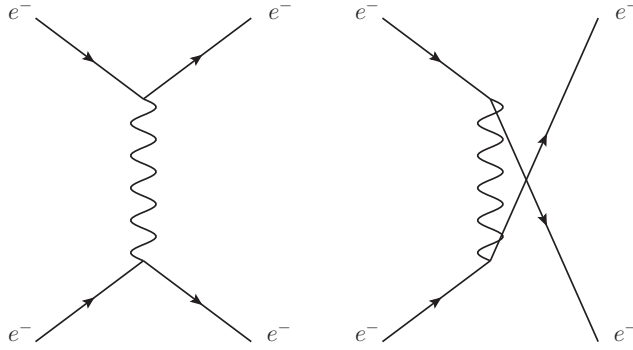


FIG. 3: Feynman diagrams for Møller scattering, $e^-e^- \rightarrow e^-e^-$, in the t (left) and u (right) channels.

Therefore, we see that MaxEnt is realized when the scattering angle is $\theta = \pi/2$, that is, when the muon-antimuon are scattered perpendicularly to the original direction of motion of the electron and positron.

2. Møller scattering: $e^-e^- \rightarrow e^-e^-$

The next process that we consider is Møller scattering, $e^-e^- \rightarrow e^-e^-$, electron-electron elastic scattering. The main difference as compared to $e^+e^- \rightarrow \mu^+\mu^-$ scattering is that there is no s -channel diagram. Tree-level Møller scattering is mediated instead by t and u -channel diagrams, as illustrated in Fig. 3. This process illustrates a different way of realizing MaxEnt from an initial product state, by means of the the interference between t and u channels.

To analyze the way this mechanism for entanglement generation works, we write the scattering amplitudes in the helicity basis for the two Feynman diagrams in terms of the t and u Mandelstam variables. The result for initial product states that share the same helicity reads

$$\begin{aligned}
 \mathcal{M}_{|RR\rangle \rightarrow |RR\rangle} &= \mathcal{M}_{|LL\rangle \rightarrow |LL\rangle} = -\frac{2\left((t+u)^3 - 2m_e^2(t^2+u^2)\right)}{tu(t+u)}, \\
 \mathcal{M}_{|RR\rangle \rightarrow |LL\rangle} &= \mathcal{M}_{|LL\rangle \rightarrow |RR\rangle} = -\frac{8m_e^2}{(t+u)}, \\
 \mathcal{M}_{|RR\rangle \rightarrow |RL\rangle} &= -\mathcal{M}_{|RR\rangle \rightarrow |LR\rangle} = -\frac{2m_e(t-u)\sqrt{tu(4m_e^2-(t+u))}}{(t+u)tu}, \\
 \mathcal{M}_{|LL\rangle \rightarrow |RL\rangle} &= -\mathcal{M}_{|LL\rangle \rightarrow |LR\rangle} = -\frac{2m_e(t-u)\sqrt{tu(4m_e^2-(t+u))}}{(t+u)tu},
 \end{aligned} \tag{A6}$$

and for initial product states with opposite helicities we have instead that

$$\begin{aligned}
 \mathcal{M}_{|RL\rangle \rightarrow |RR\rangle} &= \mathcal{M}_{|RL\rangle \rightarrow |LL\rangle} = \frac{2m_e(t-u)\sqrt{tu(4m_e^2-(t+u))}}{(t+u)tu}, \\
 \mathcal{M}_{|LR\rangle \rightarrow |RR\rangle} &= \mathcal{M}_{|LR\rangle \rightarrow |LL\rangle} = -\frac{2m_e(t-u)\sqrt{tu(4m_e^2-(t+u))}}{(t+u)tu}, \\
 \mathcal{M}_{|RL\rangle \rightarrow |RL\rangle} &= \mathcal{M}_{|LR\rangle \rightarrow |LR\rangle} = -\frac{2(2m_e^2(t-u)+u(t+u))}{t(t+u)}, \\
 \mathcal{M}_{|RL\rangle \rightarrow |LR\rangle} &= \mathcal{M}_{|LR\rangle \rightarrow |RL\rangle} = -\frac{2(2m_e^2(t-u)-t(t+u))}{u(t+u)}.
 \end{aligned} \tag{A7}$$

Using these helicity scattering amplitudes, we can now compute the concurrences for the two relevant cases: an incoming product state where the two fermions share the same helicity, or where the incoming fermions have opposite helicities. The value of these concurrences, valid for any value of the center-of-mass energy (not only in the high-energy

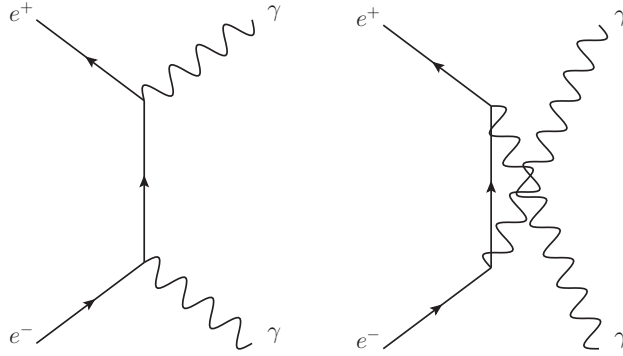


FIG. 4: Feynman diagrams for pair annihilation to photons, $e^-e^+ \rightarrow \gamma\gamma$, in the t (left) and u (right) channels.

approximation) turn out to be given by:

$$\Delta_{RR} = \left| \frac{2m_e^2 tu ((3t+u)(t+3u) - 4m_e^2(t+u))}{(t+u)^5 - 2m_e^2(2t^4 + 5t^3u + 2t^2u^2 + 5tu^3 + 2u^4) + 4m_e^4(t+u)(t^2+u^2)} \right|, \quad (\text{A8})$$

$$\Delta_{RL} = \left| \frac{2tu (tu(t+u) + m_e^2(t-u)^2)}{2m_e^2(t-u)^2(2m_e^2(t+u) - (2t^2 + 3tu + 2u^2)) + (t+u)(t^4 + u^4)} \right|. \quad (\text{A9})$$

Recalling the fact that the kinematical condition $u = t$ corresponds to an scattering angle of $\theta = \pi/2$, we obtain that for this configuration

$$\Delta_{RR} \xrightarrow{u=t} \frac{m_e^2(m_e^2 - 2t)}{m_e^4 - 2m_e^2t + 2t^2} \xrightarrow{t \ll m_e} 1 + \mathcal{O}\left(\frac{t^2}{m_e^4}\right), \quad (\text{A10})$$

$$\Delta_{RL} \xrightarrow{u=t} 1. \quad (\text{A11})$$

Therefore, we find that in Møller scattering MaxEnt is realized at a scattering angle $\theta = \pi/2$ for all energies provided that the incoming particles have opposite helicities. On the other hand, the same analysis also implies that for product states composed by same-helicity particles, MaxEnt is only realized at very low energies, well below the electron mass.

3. Pair annihilation to photons: $e^-e^+ \rightarrow \gamma\gamma$

This process is another example of indistinguishability as a basic source of entanglement. Note that pair annihilation to two photons is also described by the combination of t and u channels, as was the case for Møller scattering (see Fig. 4). The final-state photons can be expressed in the circular polarization basis, defined as follows:

$$\epsilon_\lambda(\theta, \phi) = \frac{\lambda}{\sqrt{2}} (0, \cos\theta \cos\phi + i\lambda \sin\phi, \cos\theta \sin\phi - i\lambda \cos\phi, -\sin\theta), \quad (\text{A12})$$

$$|R\rangle \equiv \epsilon_{\lambda=+1}(\theta, \phi) \quad |L\rangle \equiv \epsilon_{\lambda=-1}(\theta, \phi) \quad (\text{A13})$$

The helicity scattering amplitudes in terms of the Mandelstam variables u and t are:

$$\begin{aligned} \mathcal{M}_{|RR\rangle \rightarrow |RR\rangle} &= -\mathcal{M}_{|LL\rangle \rightarrow |LL\rangle} = -\frac{m(t+u-2m^2)}{(m^2-t)(m^2-u)} \left(\sqrt{2m^2-(t+u)} - \sqrt{-2m^2-(t+u)} \right), \\ \mathcal{M}_{|RR\rangle \rightarrow |LL\rangle} &= -\mathcal{M}_{|LL\rangle \rightarrow |RR\rangle} = \frac{m(t+u-2m^2)}{(m^2-t)(m^2-u)} \left(\sqrt{2m^2-(t+u)} + \sqrt{-2m^2-(t+u)} \right), \\ \mathcal{M}_{|RR\rangle \rightarrow |RL\rangle} &= \mathcal{M}_{|RR\rangle \rightarrow |LR\rangle} = -\frac{4m(m^4-tu)}{(m^2-t)(m^2-u)\sqrt{-2m^2-(t+u)}}, \\ \mathcal{M}_{|LL\rangle \rightarrow |RL\rangle} &= \mathcal{M}_{|LL\rangle \rightarrow |LR\rangle} = -\mathcal{M}_{|RR\rangle \rightarrow |RL\rangle}, \end{aligned} \quad (\text{A14})$$

and

$$\begin{aligned}
\mathcal{M}_{|RL\rangle\rightarrow|RL\rangle} &= \mathcal{M}_{|RL\rangle\rightarrow|LR\rangle} = \mathcal{M}_{|LR\rangle\rightarrow|RL\rangle} = \mathcal{M}_{|LR\rangle\rightarrow|LR\rangle} = 0, \\
\mathcal{M}_{|RL\rangle\rightarrow|LR\rangle} &= \mathcal{M}_{|LR\rangle\rightarrow|LR\rangle} = \sqrt{\frac{tu - m^4}{(t+u)^2 - 4m^4}} \frac{\sqrt{(t+u)^2 - 4m^4}(u-t) - (4m^4 - (t+u)^2)}{(m^2-t)(m^2-u)\sqrt{1 + \frac{4m^2}{(t+u)-2m^2}}}, \\
\mathcal{M}_{|RL\rangle\rightarrow|LR\rangle} &= \mathcal{M}_{|LR\rangle\rightarrow|RL\rangle} = \sqrt{\frac{tu - m^4}{(t+u)^2 - 4m^4}} \frac{\sqrt{(t+u)^2 - 4m^4}(u-t) + (4m^4 - (t+u)^2)}{(m^2-t)(m^2-u)\sqrt{1 + \frac{4m^2}{(t+u)-2m^2}}}.
\end{aligned} \tag{A15}$$

The corresponding concurrences are then given by

$$\begin{aligned}
\Delta_{RR} &= \left| \frac{2m^2(4m^6 - 4m^4(t+u) - 2m^2(t-u)^2 + (t+u)^3) - 8t^2u^2}{4m^4(2m^4 + 2m^2(t+u) - (t^2 + 6tu + u^2)) + t^4 + 4t^3u + 14t^2u^2 + 4tu^3 + u^4} \right|, \\
\Delta_{RL} &= \frac{2(tu - m^4)}{t^2 + u^2 - 2m^4}.
\end{aligned} \tag{A16}$$

As in the case of Møller scattering, if $\theta = \pi/2$ (corresponding to $t = u$) MaxEnt is realized for all energies when the initial particles have opposite helicities, while MaxEnt arises only for small momentum transfers t in the case in which the initial-state particles share the same helicity,

$$\Delta_{RR} \xrightarrow{u=t} \frac{(m^2 - t)}{m^2 + 3t} \xrightarrow{t \ll m_e} 1 + \mathcal{O}\left(\frac{t}{m_e^2}\right), \tag{A17}$$

$$\Delta_{RL} \xrightarrow{u=t} 1 \forall t. \tag{A18}$$

Appendix B: Unconstrained QED

In this appendix we provide more information about unconstrained QED (uQED) and about the form of the helicity scattering amplitudes computed in this hypothetical theory. The Dirac matrices γ^μ form the Clifford algebra of the 4×4 matrices; $\{\gamma^\mu, \gamma^\nu\} = 2g^{\mu\nu}$ if the metric is $(+, -, -, -)$. The complexification of the Clifford algebra $\mathcal{Cl}_{1,3}(\mathbf{R})$, $\mathcal{Cl}_{1,3}(\mathbf{R})_{\mathbf{C}}$, is isomorphic to the algebra of 4×4 complex matrices. Therefore, it is possible to express any general 4×4 complex matrix as

$$G^\mu = c_1^\mu \mathbb{I} + c_2^{\mu\nu} \gamma_\nu + ic_3^\mu \gamma^5 + c_4^{\mu\nu} \gamma^5 \gamma_\nu + c_5^{\mu\nu\rho} \sigma_{\nu\rho}, \tag{B1}$$

where the expansion coefficients are real-valued, $c_i \in \mathbb{R}$, and $\gamma^5 = i\gamma^0\gamma^1\gamma^2\gamma^3$, $\sigma^{\nu\rho} = -\frac{i}{2}[\gamma^\nu, \gamma^\rho]$. The hypothetical theory of unconstrained QED is constructed by replacing the QED vertex $-ie\gamma^\mu$ by the general 4×4 complex matrices $-ieG^\mu$. To simplify the analysis, we first impose the conservation of the C, P and T discrete symmetries, which leads to $c_1^\mu = c_3^\mu = c_4^{\mu\nu} = c_5^{\mu\nu\rho} = 0$ and $c_2^{\mu\nu} \equiv a^{\mu\nu}$ with $a^{i0} = a^{0j} = 0$ for $i, j = 1, 2, 3$.

With these assumptions for the electron-photon interaction vertex, when computing the amplitudes at high energy limit for the process $e^+e^- \rightarrow \mu^+\mu^-$ using and restricting the particles to be in the XZ plane one obtains the following results for incoming $|RL\rangle$:

$$\begin{aligned}
\mathcal{M}_{|RL\rangle\rightarrow|RL\rangle} &= -a_{j2}^2 - a_{j1}^2 \cos\theta + a_{j1}a_{j3} \sin\theta + i(a_{j1}a_{j2}(1 - \cos\theta) + a_{j2}a_{j3} \sin\theta), \\
\mathcal{M}_{|RL\rangle\rightarrow|LR\rangle} &= a_{j2}^2 - a_{j1}^2 \cos\theta + a_{j1}a_{j3} \sin\theta - i(a_{j1}a_{j2}(1 + \cos\theta) - a_{j2}a_{j3} \sin\theta),
\end{aligned} \tag{B2}$$

while all other scattering amplitudes vanish.

The two possible final states that maximize the concurrence, that is, that realize MaxEnt are given by $|RL\rangle \pm |LR\rangle$, and therefore $\mathcal{M}_{|RL\rangle\rightarrow|RL\rangle} = \pm \mathcal{M}_{|RL\rangle\rightarrow|LR\rangle}$. Requiring a final state that satisfies the maximal entanglement principle we find that for a scattering angle of $\theta = \pi/2$ the following conditions must be satisfied

$$\begin{aligned}
a_{j2}^2 - ia_{j1}a_{j2} = 0 &\longrightarrow A_{22} = A_{12} = 0 \text{ if } \mathcal{M}_{|RL\rangle} = \mathcal{M}_{|LR\rangle} \text{ or} \\
a_{j1}a_{j3} + ia_{j2}a_{j3} = 0 &\longrightarrow A_{13} = A_{23} = 0 \text{ if } \mathcal{M}_{|RL\rangle} = -\mathcal{M}_{|LR\rangle},
\end{aligned} \tag{B3}$$

where $A_{kl} \equiv a_{jk}a_{jl}$ is a positive definite matrix. It is also possible to redo the same analysis but now requiring the scattered particles to lie in the YZ and XY planes respectively. If the motion of the initial particles takes place in

the Y axis and the outgoing scattered particles lie in the YZ plane, the corresponding scattering amplitudes become:

$$\begin{aligned}\mathcal{M}_{|RL\rangle\rightarrow|RL\rangle} &= -a_{j1}^2 - a_{j2}^2 \cos \theta + a_{j2}a_{j3} \sin \theta - i(a_{j1}a_{i2}(1 - \cos \theta) + a_{j1}a_{j3} \sin \theta), \\ \mathcal{M}_{|RL\rangle\rightarrow|LR\rangle} &= a_{j1}^2 - a_{j2}^2 \cos \theta + a_{j2}a_{j3} \sin \theta + i(a_{j1}a_{j2}(1 + \cos \theta) - a_{j1}a_{j3} \sin \theta).\end{aligned}\quad (\text{B4})$$

If now we request MaxEnt to be realized at an scattering angle of $\theta = \pi/2$, one finds that

$$\begin{aligned}a_{j1}^2 + ia_{j1}a_{j2} = 0 &\longrightarrow A_{11} = A_{12} = 0 \text{ if } \mathcal{M}_{|RL\rangle} = \mathcal{M}_{|LR\rangle} \text{ or} \\ a_{j2}a_{j3} - ia_{j1}a_{j3} = 0 &\longrightarrow A_{23} = A_{13} = 0 \text{ if } \mathcal{M}_{|RL\rangle} = -\mathcal{M}_{|LR\rangle}.\end{aligned}\quad (\text{B5})$$

For incoming particles in X axis and outgoing in the XY plane, the results read instead

$$\begin{aligned}\mathcal{M}_{|RL\rangle\rightarrow|RL\rangle} &= -a_{j3}^2 - a_{j2}^2 \cos \phi + a_{j1}a_{j2} \sin \phi + i(a_{j2}a_{i3}(1 - \cos \phi) + a_{j1}a_{j3} \sin \phi), \\ \mathcal{M}_{|RL\rangle\rightarrow|LR\rangle} &= -a_{j3}^2 + a_{j2}^2 \cos \phi - a_{j1}a_{j2} \sin \phi + i(a_{j2}a_{j3}(1 + \cos \phi) - a_{j1}a_{j3} \sin \phi).\end{aligned}\quad (\text{B6})$$

where ϕ is the azimuthal angle that goes from 0 to 2π . Fixing $\phi = \pi/2$ we get another set of conditions

$$\begin{aligned}a_{j1}a_{j2} + ia_{j1}a_{j3} = 0 &\longrightarrow A_{12} = A_{13} = 0 \text{ if } \mathcal{M}_{|RL\rangle} = \mathcal{M}_{|LR\rangle} \text{ or} \\ a_{j3}^2 - ia_{j2}a_{j3} = 0 &\longrightarrow A_{23} = A_{33} = 0 \text{ if } \mathcal{M}_{|RL\rangle} = -\mathcal{M}_{|LR\rangle}.\end{aligned}\quad (\text{B7})$$

A crucial property of entanglement is that it should be invariant under local unitary transformations like rotations. For this reason, it is possible to obtain the $|RL\rangle + |LR\rangle$ state in one plane and $|RL\rangle - |LR\rangle$ state in another, but both for the same scattering angle because of isometry. Therefore, there are a finite number of possible solutions that satisfy the above constraints: the one which corresponds to QED is the $|RL\rangle - |LR\rangle$ state for XZ and YZ plane and $|RL\rangle + |LR\rangle$ state for XY plane. While in this example we have imposed that MaxEnt is realized for specific choices of the scattering angles $\theta, \phi = \pi/2$, it is conceivable that additional constraints could be obtained by exploiting the information contained in other scattering angles.

From this specific example among the list of processes that we have analyzed in unconstrained QED, one can also observe that it is not possible to distinguish the overall sign of the a_{ij} coefficients, as they always appear squared or multiplied in pairs. Other processes, involving for example a final state with three particles, might be necessary in order to resolve this degeneracy.

Notice also that uQED allows angular momentum violation. Let us take as example the amplitudes for the process $e^+e^- \rightarrow \mu^+\mu^-$ in the XZ plane. The results for an initial state $|RL\rangle$ are collected in Eq. (B2), whereas the corresponding amplitudes for an initial state $|LR\rangle$ read

$$\begin{aligned}\mathcal{M}_{|LR\rangle\rightarrow|RL\rangle} &= -a_{j2}^2 + a_{j1}^2 \cos \theta - a_{j1}a_{j3} \sin \theta + i(-a_{j1}a_{j2}(1 + \cos \theta) + a_{j2}a_{j3} \sin \theta), \\ \mathcal{M}_{|LR\rangle\rightarrow|LR\rangle} &= a_{j2}^2 + a_{j1}^2 \cos \theta - a_{j1}a_{j3} \sin \theta + i(a_{j1}a_{j2}(-1 + \cos \theta) - a_{j2}a_{j3} \sin \theta).\end{aligned}\quad (\text{B8})$$

Therefore, if the initial state is $|\Psi^-\rangle = \frac{1}{\sqrt{2}}(|RL\rangle - |LR\rangle)$, i.e. the singlet state, then the final state $|\psi\rangle_{\text{final}}$ becomes

$$\begin{aligned}|\psi\rangle_{\text{final}} &\sim \mathcal{M}_{|RL\rangle\rightarrow|RL\rangle}|RL\rangle + \mathcal{M}_{|RL\rangle\rightarrow|LR\rangle}|LR\rangle - (\mathcal{M}_{|LR\rangle\rightarrow|RL\rangle}|RL\rangle + \mathcal{M}_{|LR\rangle\rightarrow|LR\rangle}|LR\rangle) \\ &\sim \left(-\sum_j a_{j1}^2 \cos \theta + \sum_j a_{j1}a_{j3} \sin \theta \right) (|RL\rangle - |LR\rangle) + i \sum_j a_{j1}a_{j2} (|RL\rangle + |LR\rangle),\end{aligned}\quad (\text{B9})$$

which, in general, is not a singlet state: as long as $\sum_j a_{j1}a_{j2} \neq 0$, angular momentum is violated in this process $\forall \theta$.

Appendix C: Electroweak processes with helicity dependence

Finally, we provide in this appendix explicit expressions for tree-level electroweak processes with helicity dependence, first for the Z decay into e^-e^+ , and then for the $e^-e^+ \rightarrow \mu^-\mu^+$ process including the effects of Z/γ interference

1. Z decay into e^-e^+

We now analyse the helicity structure of Z boson decay to e^-e^+ . As Z is a massive particle, it has three possible polarizations: right- and left-handed circular polarizations, and longitudinal polarization, which we will denote as $|0\rangle$.

As $m_e \ll m_Z$ we can neglect the electron mass. The non-vanishing helicity amplitudes for this decay process are:

$$\begin{aligned}
\mathcal{M}_{|0\rangle\rightarrow|RL\rangle} &= g_R m_Z \sin \theta, \\
\mathcal{M}_{|0\rangle\rightarrow|LR\rangle} &= g_L m_Z \sin \theta, \\
\mathcal{M}_{|R\rangle\rightarrow|RL\rangle} &= g_R m_Z \sqrt{2} \sin^2(\theta/2), \\
\mathcal{M}_{|R\rangle\rightarrow|LR\rangle} &= -g_L m_Z \sqrt{2} \cos^2(\theta/2), \\
\mathcal{M}_{|L\rangle\rightarrow|RL\rangle} &= g_R m_Z \sqrt{2} \cos^2(\theta/2), \\
\mathcal{M}_{|L\rangle\rightarrow|LR\rangle} &= -g_L m_Z \sqrt{2} \sin^2(\theta/2),
\end{aligned} \tag{C1}$$

where we have defined $g_R = (g_V - g_A)/2$ and $g_L = (g_V + g_A)/2$.

If the Z boson is longitudinally polarized, the concurrence of the final leptons becomes

$$\Delta_0 = \frac{2|g_L g_R|}{g_L^2 + g_R^2}, \tag{C2}$$

Then one can see that the leptons pair is maximally entangled provided that $|g_L| = |g_R|$, *i.e.* if $g_A = 0$ or $g_V = 0$. As $g_A = T_3/2 \neq 0$ the only possible solution is $g_V = 0$ which leads to the value $\theta_W = \pi/6$ of the weak mixing angle.

For a Z boson initially polarized with either a right- or left-handed polarization, the concurrence becomes instead

$$\Delta_R = \frac{2|g_L g_R| \sin^2 \theta}{|2(g_L^2 - g_R^2) \cos \theta + (g_L^2 + g_R^2)(1 + \cos^2 \theta)|}, \tag{C3}$$

$$\Delta_L = \frac{2|g_L g_R| \sin^2 \theta}{|2(g_L^2 - g_R^2) \cos \theta - (g_L^2 + g_R^2)(1 + \cos^2 \theta)|}. \tag{C4}$$

We already showed in Fig. 1 the dependence of g_R/g_L for the maximum concurrence as a function of scattering angle θ . As long as $g_R/g_L = \pm \cot^2(\theta/2)$, for an initial right-handed polarization, or $g_R/g_L = \pm \tan^2(\theta/2)$, for an initial left-handed polarization, MaxEnt is achieved. However, if we assume the same relation between g_R/g_L independently of the initial polarization, then only one solution is possible: $g_R/g_L = \pm 1$, *i.e.* the same solution as for longitudinal polarization, $g_V = 0$ or equivalently $\theta_W = \pi/6$.

2. $e^- e^+ \rightarrow \mu^- \mu^+$ with Z/γ interference

We now revisit the $e^- e^+ \rightarrow \mu^- \mu^+$ scattering processes, now taking into account the effects of Z/γ interference. Given that $m_e, m_\mu \ll m_Z$, we can neglect the masses of both leptons. In this process, the equal initial helicity amplitudes vanish, while the scattering amplitudes for the opposite helicity initial configurations are given by:

$$\begin{aligned}
\mathcal{M}_{|RL\rangle\rightarrow|RL\rangle} &= - \left(\frac{4\mu^2 g_R^2}{(4\mu^2 - 1)} \sec^2 \theta_W + Q^2 \sin^2 \theta_W \right) (1 + \cos \theta), \\
\mathcal{M}_{|RL\rangle\rightarrow|LR\rangle} &= \left(\frac{4\mu^2 g_R g_L}{(4\mu^2 - 1)} \sec^2 \theta_W + Q^2 \sin^2 \theta_W \right) (1 - \cos \theta), \\
\mathcal{M}_{|LR\rangle\rightarrow|RL\rangle} &= \mathcal{M}_{|RL\rangle\rightarrow|LR\rangle} (g_R \leftrightarrow g_L), \\
\mathcal{M}_{|LR\rangle\rightarrow|LR\rangle} &= \mathcal{M}_{|RL\rangle\rightarrow|RL\rangle} (g_R \leftrightarrow g_L),
\end{aligned} \tag{C5}$$

where we have defined $\mu \equiv |\vec{p}|/m_Z$.

We can analyse the purely weak scattering process $e^- e^+ \rightarrow \mu^- \mu^+$, *i.e.*, where the two currents exchange a Z boson instead of a photon like in QED. In this case, we can set $Q = 0$ in the amplitudes of Eq. (C6). In the high-energy limit $\mu \rightarrow \infty$, the concurrences become

$$\Delta_{RL} = \frac{|g_L g_R| \sin^2 \theta}{2(g_R^2 \cos^4(\theta/2) + g_L^2 \sin^4(\theta/2))}, \tag{C6}$$

$$\Delta_{LR} = \frac{|g_L g_R| \sin^2 \theta}{2(g_L^2 \cos^4(\theta/2) + g_R^2 \sin^4(\theta/2))}. \tag{C7}$$

Therefore, as discussed in Sect. V, depending on the specific initial helicities of the particles, the angular dependence for maximal concurrence is different. However, MaxEnt is present at the same scattering angle when $|g_R| = |g_L|$ as happens in Z decay. In fact, it is the same angular dependence and Fig. 1 also applies for this scattering process.

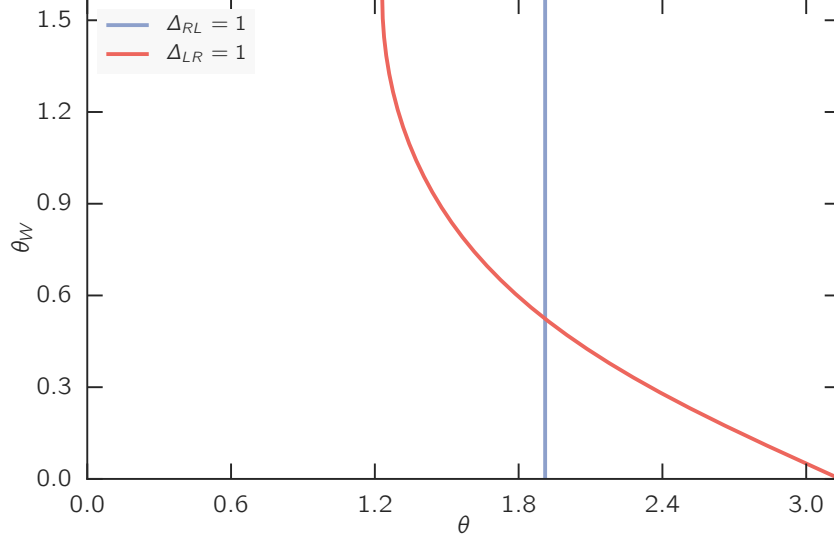


FIG. 5: Maximum concurrence line for the weak mixing angle θ_W as a function of scattering angle θ for the process $e^-e^+ \rightarrow \mu^-\mu^+$ including the effects of Z/γ interference. If the e^- (e^+) has a right(left)-handed helicity, MaxEnt is possible as long as $\theta = \arccos(-1/3)$, whereas if they have left(right)-handed helicity there is a dependence between θ_w and θ . However, if we impose that MaxEnt needs to be achieved for the same value of the scattering angle θ , then $\Delta_{LR} = 1$ fixes that $\theta_W = \pi/6$.

If we include the effects of the photon/ Z interference, the expression for the concurrences become more complicated. They simplify if we express them in terms of Q and T_3 , in which case we find

$$\Delta_{RL} = \frac{2Q(Q - T_3) \sin^2 \theta}{2(2Q - T_3)T_3 \cos \theta + ((Q - T_3)^2 + Q^2)(1 + \cos^2 \theta)}, \quad (\text{C8})$$

$$\Delta_{LR} = \frac{Q(Q - T_3) \sin^2 \theta \sin^2 \theta_W (T_3^2 + Q^2 \sin^2 \theta_W - 2QT_3 \sin^2 \theta_W)}{2Q^2(Q - T_3)^2 \sin^4(\theta/2) \sin^4 \theta_W + 2(T_3^2 + Q^2 \sin^2 \theta_W - 2QT_3 \sin^2 \theta_W)^2 \cos^4(\theta/2)}.$$

Note that Δ_{RL} does not depend on the weak mixing angle, but Δ_{LR} does. Taking the appropriate values for the leptonic electric and weak isospin charges, $Q = -1$ and $T_3 = -1/2$, we find that

$$\Delta_{RL} = \frac{4 \sin^2 \theta}{6 \cos \theta + 5(1 + \cos^2 \theta)}, \quad (\text{C9})$$

$$\Delta_{LR} = \frac{\sin^2 \theta \sin^2 \theta_W}{\cos^4(\theta/2) + 4 \sin^4(\theta/2) \sin^4 \theta_W}. \quad (\text{C10})$$

Therefore, requesting that MaxEnt is realized implies that

$$\theta(\Delta_{RL} = 1) = \arccos\left(-\frac{1}{3}\right) \forall \theta_W, \quad (\text{C11})$$

$$\theta_W(\Delta_{LR} = 1) = \arcsin\left(\frac{1}{\sqrt{2}} \cot(\theta/2)\right). \quad (\text{C12})$$

The two curves are shown in Fig. 5. If MaxEnt is realized for the same scattering angle independently of the specific scattering initial state, then the prediction $\theta_W = \pi/6$ readily follows, consistently with the result that we find by requesting MaxEnt in the decays of the Z boson into leptons.

[1] E. Schrödinger, Math. Proc. Cambridge Philosophical Society. 31(4), 555 (1935),

- [2] J. S. Bell, *Physics* 1, 195 (1964).
A. Aspect, P. Grangier and G. Roger, *Phys. Rev. Lett.* 47 460 (1981).
- [3] Artur K. Ekert, *Phys. Rev. Lett.* 67, 661 (1991).
- [4] C. H. Bennett, G. Brassard, C. Crpeau, R. Jozsa, A. Peres and W. K. Wootters, *Phys. Rev. Lett.* 70, 1895 (1993).
- [5] P. Shor, *SIAM J.Sci.Statist.Comput.* 26 (1997) 1484.
- [6] C. Holzhey, F. Larsen and F. Wilczek, *Nucl. Phys. B* 424,443 (1994).G. Vidal, J. I. Latorre, E. Rico and A. Kitaev, *Phys. Rev. Lett.* 90, 227902 (2003).P. Calabrese and J. Cardy, *J.Stat.Mech.*0406:P06002 (2004).
- [7] A. Acín, J. I. Latorre and P. Pascual, *Phys. Rev. A* **63**, 042107 (2001).
- [8] R. A. Bertlmann and B. C. Hiesmayr, *Quantum Inf. Process.* **5** 421-440 (2006).
B. C. Hiesmayr, *Sci. Rep.* **5** (2015) 11591.
- [9] J. Bernabeu, *J. Phys. Conf. Ser.* 335, 012011 (2011).
- [10] S. Barnerjee, A. K. Alok, R. Srikanth and B. C. Hiesmayr, *EPJ C* **75** 487 (2015).
- [11] R. Peschanski and S. Seki, *Phys. Lett.* B758 (2016).
- [12] D. E. Kharzeev and E. M. Levin, [arxiv.org/1702.03489](https://arxiv.org/abs/1702.03489).
- [13] J. Maldacena, *Fortsch. Phys.* 64, 10 (2016).
- [14] S. Hill and W. K. Wootters, *Phys.Rev.Lett.*78, 5022 (1997).
- [15] C. Patrignani *et al.* [Particle Data Group], *Chin. Phys. C* **40**, no. 10, 100001 (2016).
- [16] J. A. Wheeler, *Complexity, Entropy, and the physics of Information* (1990).